
Fundamentals of **MICROFABRICATION**

Marc Madou



CRC Press
Boca Raton New York

Development Editor: Marleen Madou
Publisher: Ron Powers
Project Editor: Paul Gottehrer
Prepress: Gary Bennett, Kevin Luong, Carlos Esser, Walt Cerny, Greg Cuciak
Cover design: Denise Craig

Library of Congress Cataloging-in-Publication Data

Madou, Marc J.
Fundamentals of microfabrication / Marc Madou.
p. cm.
Includes bibliographical references and index.
ISBN 0-8493-9451-1 (alk. paper)
1. Microelectronics—Design and construction. 2. Machining.
3. Microelectronic packaging. 4. Lasers—Industrial applications.
I. Title.
TK7836.M33 1997
621.3815'2—dc20

SC1
TK
7836
.M33
1997

96-43344
CIP

This book contains information obtained from authentic and highly regarded sources. Reprinted material is quoted with permission, and sources are indicated. A wide variety of references are listed. Reasonable efforts have been made to publish reliable data and information, but the author and the publisher cannot assume responsibility for the validity of all materials or for the consequences of their use.

Neither this book nor any part may be reproduced or transmitted in any form or by any means, electronic or mechanical, including photocopying, microfilming, and recording, or by any information storage or retrieval system, without prior permission in writing from the publisher.

The consent of CRC Press LLC does not extend to copying for general distribution, for promotion, for creating new works, or for resale. Specific permission must be obtained in writing from CRC Press LLC for such copying.

Direct all inquiries to CRC Press LLC, 2000 Corporate Blvd., N.W., Boca Raton, Florida 33431.

© 1997 by CRC Press LLC

No claim to original U.S. Government works

International Standard Book Number 0-8493-9451-1

Library of Congress Card Number 96-43344

Printed in the United States of America 1 2 3 4 5 6 7 8 9 0

Printed on acid-free paper

sition process. The stress turns from tensile in stoichiometric films to compressive in silicon-rich films (for details see Chapter 5). A great number of materials are not attacked by anisotropic etchants. Hence, a thin film of such a material can be used as an etch stop.

Another example is the SiO_2 layer in a silicon-on-insulator structure (SOI). A buried layer of SiO_2 , sandwiched between two layers of crystalline silicon, forms an excellent etch stop because of the good selectivity of many etchants of Si over SiO_2 . The oxide does not exhibit the good mechanical properties of silicon nitride and is consequently used rarely as a mechanical member in a microdevice. As with the photo-induced preferential anodization (PiPA), no metal contacts are needed with an SOI etch stop, greatly simplifying the process over an electrochemical etch stop technique.

We have classified SOI micromachining under surface micromachining in Chapter 5. More details about this very promising micromachining alternative are presented there.

Problems with Wet Bulk Micromachining

Introduction

Despite the introduction of better controllable etch-stop techniques, bulk micromachining remains a difficult industrial process to control. It is also not an applicable submicron technology, because wet chemistry is not able to etch reliably on that scale. For submicron structure definition dry etching is required (dry etching is also more environmentally safe). We will look now into some of the other problems associated with bulk micromachining, such as the extensive real estate con-

sumption and difficulties in etching at convex corners, and detail the solutions that are being worked on to avoid, control, or alleviate those problems.

Extensive Real Estate Consumption

Introduction

Bulk micromachining involves extensive real estate consumption. This quickly becomes a problem in making arrays of devices. Consider the diagram in Figure 4.56, illustrating two membranes created by etching through a $\langle 100 \rangle$ wafer from the backside until an etch stop, say a Si_3N_4 membrane, is reached. In creating two of these small membranes a large amount of Si real estate is wasted and the resulting device becomes quite fragile.

Real Estate Gain by Etching from the Front

One solution to limiting the amount of Si to be removed is to use thinner wafers, but this solution becomes impractical below $200\ \mu\text{m}$ as such wafers break too often during handling. A more elegant solution is to etch from the front rather than from the back. Anisotropic etchants will undercut a masking material an amount dependent on the orientation of the wafer with respect to the mask. Such an etchant will etch any $\langle 100 \rangle$ silicon until a pyramidal pit is formed, as shown in Figure 4.57. These pits have sidewalls with a characteristic 54.7° angle with respect to the surface of a $\langle 100 \rangle$ silicon wafer, since the delineated planes are $\{111\}$ planes. This etch property makes it possible to form cantilever structures by etching from the front side, as the cantilevers will be undercut and eventually will be suspended over a pyramidal pit in the silicon. Once this pyramidal

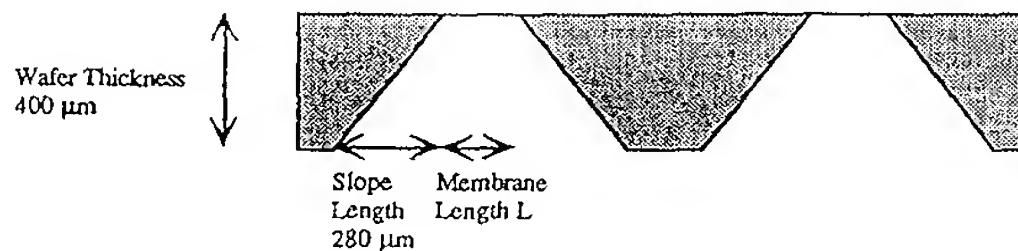


FIGURE 4.56 Two membranes formed in a $\langle 100 \rangle$ -oriented silicon wafer.

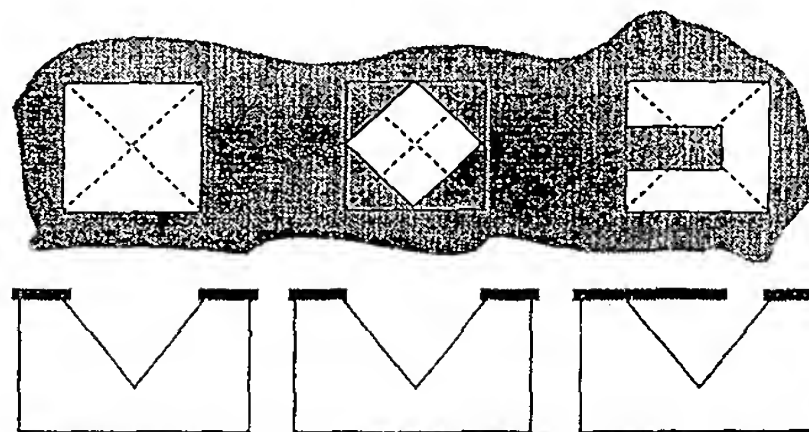


FIGURE 4.57 Three anisotropically etched pits etched from the front in a $\langle 100 \rangle$ -oriented silicon wafer.

pit is completed, the etch rate of the {111} planes exposed is extremely slow and practically stops. Process sequences, which depend on achieving this type of a final structure, are therefore very uniform across a wafer and very controllable. The upper drawings in Figure 4.57 represent patterned holes in a masking material: a square, a diamond, and a square with a protruding tab. The drawings immediately below represent the etched pit in the silicon produced by the anisotropic etchant. Note in the first drawing that the square mask produces a four-sided pyramidal pit. In the second drawing, a similar shape oriented at 45° produces an etched pit which is oriented parallel to the pit etched in the first drawing. In the second drawing the corners of the diamond are undercut by the etchant as it produces the final etch pit. The third drawing illustrates that any protruding member is eventually undercut by the anisotropic etchant, leaving a cantilever structure suspended over the etch pit.

Real Estate Gain by Using Silicon Fusion-Bonded Wafers

Using silicon fusion-bonded (SFB) wafers rather than conventional wafers also makes it possible to fabricate much smaller microsensors. The process is clarified in Figure 4.58 for the fabrication of a gauge pressure sensor.¹⁸⁷ The bottom, handle wafer has a standard thickness of $525\ \mu\text{m}$ and is anisotropically etched with a square cavity pattern. Next, the etched handle wafer is fusion bonded to a top sensing wafer (the SFB process itself is detailed in Chapter 5 dealing with surface micromachining and in Chapter 8 on packaging). The sensor wafer consists of a p-type substrate with an n-type epilayer corresponding to the required thickness of the pressure-transducing membrane. The sensing wafer is thinned all the way to the epilayer by

electrochemical etching and resistors are ion implanted. The handle wafer is ground and polished to the desired thickness. For gauge measurement, the anisotropically etched cavity is truncated by the polishing operation, exposing the backside of the diaphragm. For an absolute pressure sensor the cavity is left enclosed. With the same diaphragm dimensions and the same overall thickness of the chip, an SFB device is almost 50% smaller than a conventional machined device (see Figure 4.59).

Corner Compensation

Underetching

Underetching of a mask which contains no convex corners, i.e., corners turning outside in, in principle stems from mask misalignment and/or from a finite etching of the {111} planes. Peeters measured the widening of {111}-walled V-grooves in a (100) Si wafer after etching in 7 M KOH at $80 \pm 1^\circ$ over 24 hours as $9 \pm 0.5\ \mu\text{m}$.⁴¹ The sidewall slopes of the V-groove are a well-defined 54.74° , and the actual etch rate R_{111} is related to the rate of V-groove widening R_v through:

$$R_{111} = \frac{1}{2} \sin(54.74^\circ) R_v \quad 4.41$$

$$\text{or } R_{111} = 0.408 \cdot R_v$$

with R_{111} the etch rate in nm/min and R_v the groove widening, also in nm/min. The V-groove widening experiment then results in a R_{111} of $2.55 \pm 0.15\ \text{nm/min}$. In practice, this etch rate implies

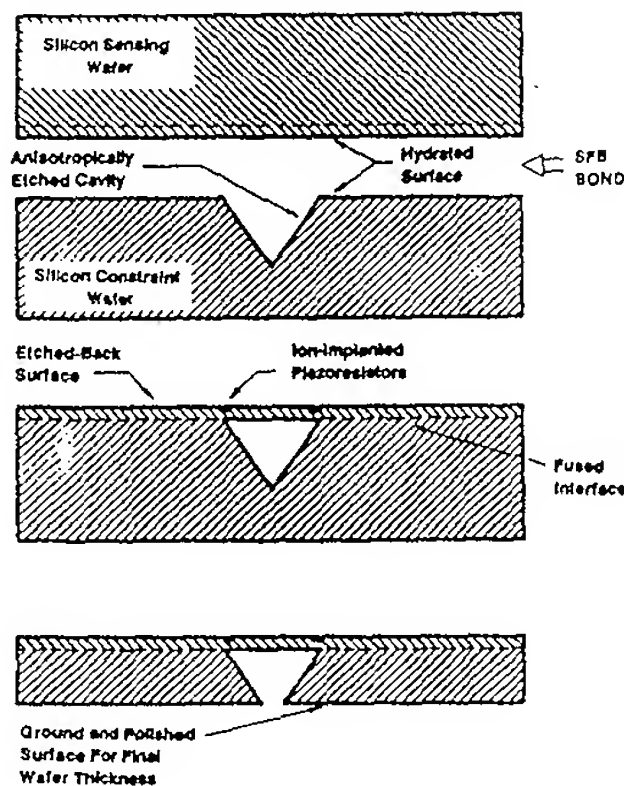


FIGURE 4.58 Fabrication process of an SFB-bonded gauge pressure sensor. (From Bryzek, J. et al., *Silicon Sensors and Microstructures*, Novasensor, Fremont, CA, 1990) With permission.)

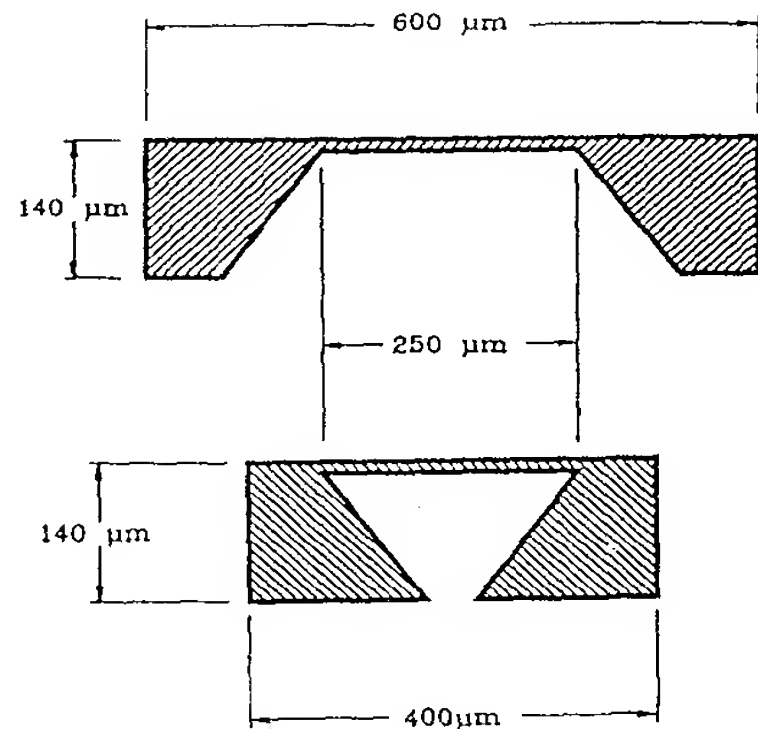


FIGURE 4.59 Comparison of conventional and SFB processes. The SFB process results in a chip which is at least 50% smaller than the conventional chip. (From Bryzek, J. et al., *Silicon Sensors and Microstructures*, Novasensor, Fremont, CA, 1990. With permission.)

a mask underetching of only $0.9\text{ }\mu\text{m}$ for an etch depth of $360\text{ }\mu\text{m}$. For a 1-mm long V-groove and a 1° misalignment angle, a total underetching of $18\text{ }\mu\text{m}$ is theoretically expected, with 95% due to misalignment and only 5% due to etching of the $\{111\}$ side-walls.⁴¹ The total underetching will almost always be determined by misalignment, rather than by etching of $\{111\}$ walls.

Mask underetching with masks that do include convex corners is usually much larger than the underetching just described, as the etchant tends to circumscribe the mask opening with $\{111\}$ walled cavities. This is usually called undercutting rather than underetching. It is advisable to avoid mask layouts with convex corners. Often mesa-type structures are essential, though, and in that case there are two possible ways to reduce the undercutting. One is by chemical additives, reducing the undercut at the expense of a reduced anisotropy ratio, and the other is by a special mask compensating the undercut at the expense of more lost real estate.

Undercutting

When etching rectangular convex corners, deformation of the edges occurs due to undercutting. This is an unwanted effect, especially in the fabrication of, say, acceleration sensors,

where total symmetry and perfect 90° convex corners on the proof mass are mandatory for good device prediction and specification. The undercutting is a function of etch time and thus directly related to the desired etch depth. An undercut ratio is defined as the ratio of undercut to etch depth (δ/H).

Saturating KOH solutions with isopropanol (IPA) reduces the convex corner undercutting; unfortunately, this happens at the cost of the anisotropy of the etchant. This additive also often causes the formation of pyramidal or cone-shaped hillocks.^{41,109} Peeters claims that these hillocks are due to carbonate contamination of the etchant and he advises etching under inert atmosphere also and stock-piling all etchant ingredient under an inert nitrogen atmosphere.⁴¹

Undercutting can also be reduced or even prevented by so-called corner compensation structures which are added to the corners in the mask layout. Depending on the etching solution, different corner compensation schemes are used. Commonly used are square corner compensation (EDP or KOH) and rotated rectangle corner compensation methods (KOH). In Figure 4.60, these two compensation methods are illustrated. In the square corner compensation case, the square of SiO_2 in the mask, outlining the square proof mass feature for an accelerometer, is

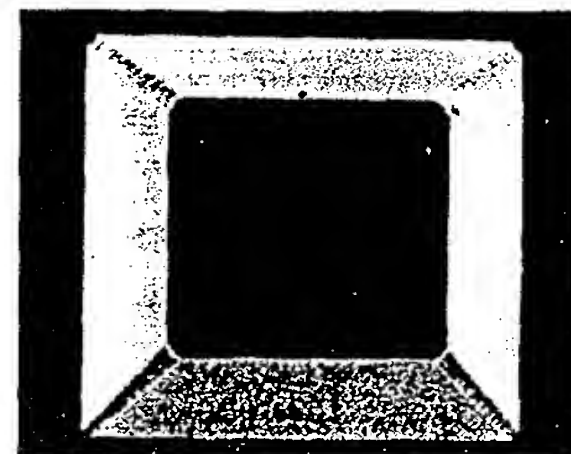
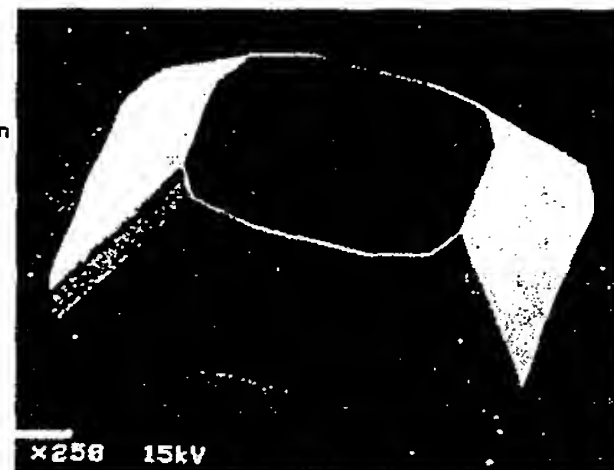
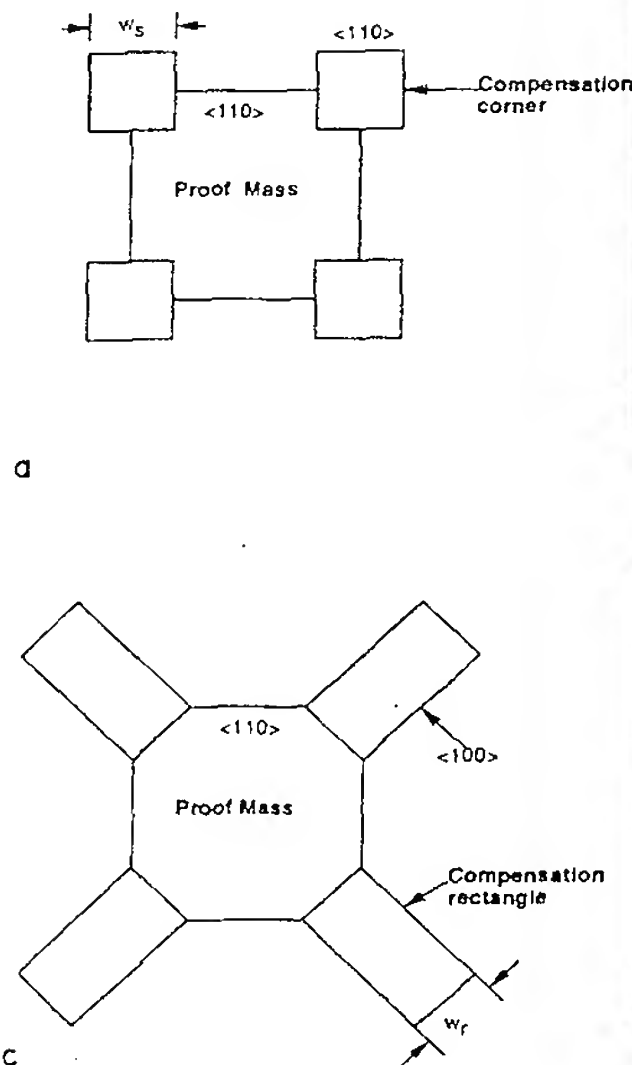


FIGURE 4.60 Formation of a proof mass by silicon bulk micromachining. (a,b) Square corner compensation method, using EDP as the etchant. (c,d) Rotated rectangle corner compensation method, using KOH as the etchant.

enhanced by adding an extra SiO_2 square to each corner (Figure 4.60a). Both the proof mass and the compensation squares are aligned with their sides parallel to the $\langle 110 \rangle$ direction. In this way, two concave corners are created at the convex corner to be protected. Thus, direct undercutting is prevented. The three 'sacrificial' convex corners at the protective square are undercut laterally by the fast etching planes during the etch process. The dimension of the compensation square, w_s , for a 500- μm thick wafer (4-in.) is about 500 μm . The resulting mesa structure after EDP or KOH etching is shown in Figure 4.60b. In the rotated rectangle corner compensation method shown in Figure 4.60c, a properly scaled rectangle (w_r should be twice the thickness of the wafer) is added to each of the mask corners. The four sides of the mesa square are still aligned along the $\langle 110 \rangle$ direction, but the compensation rectangles are rotated (45°) with their longer sides along the $\langle 100 \rangle$ directions. Using KOH as an etchant reveals the mesa shown in Figure 4.60d. A proof mass is frequently dislodged by simultaneously etching from the front and the back. Corner compensation requires significant amount of space around the corners, making the design less compact, and the method is often only applicable for simple geometries.

Different groups around the world have been using different corner compensation schemes and they all claim to have optimized spatial requirements. For an introduction to corner compensation, refer to Puers et al.¹⁸⁸ Sandmaier et al.¹⁸⁹ for KOH etching use $\langle 110 \rangle$ -oriented beams, $\langle 110 \rangle$ -oriented squares, and $\langle 010 \rangle$ -oriented bands for corner compensation. They found that spatial requirements for compensation structures could be reduced dramatically by combining several of these compensation structures. The mask layouts for some of the different compensation schemes used by Sandmaier et al. are shown in Figure 6.61. To understand the choice and dimensioning of these compensation structures, as well as those in Figure 6.60, we will first look at the planes emerging at convex corners during KOH etching. Mayer et al.¹⁹⁰ found that the undercutting of convex corners in pure KOH etch is determined exclusively by $\{411\}$ planes. The $\{411\}$ planes of the convex undercutting corner, as shown in Figure 4.62, are not entirely laid free, though; rugged surfaces, where only fractions of the main planes can be detected, overlap the $\{411\}$ planes under a diagonal line shown as AB in this figure. The ratio of $\{411\}$ to $\{100\}$ etching does not depend on temperature between 60 and 100°C . The value does decline with increasing KOH concentration from about 1.6 at 15% KOH to 1.3 at above 40% where the curve flattens out.¹⁹⁰ Ideally one avoids rugged surfaces and searches for well-defined planes bounding the convex corner. In Figure 4.63 it is shown how a $\langle 110 \rangle$ beam is added to the convex corner to be etched. The fast etching $\{411\}$ planes, starting at the two convex corners, are laterally undercutting a $\langle 110 \rangle$ -oriented beam (broken lines in Figure 4.63). It is clear that the longer this $\langle 110 \rangle$ -oriented beam is, the longer the convex corner is protected from undercutting. It is essential that by the end of the etch the beam has disappeared to maintain a minimum of rugged surface at the convex edge. On the other hand, as is obvious from Figure 4.63, a complete disappearance of the beam leads to a beveling at the face of the convex corner. The dimensioning of the

compensating $\langle 110 \rangle$ beam works then as follows: the length of the compensating beam is calculated primarily from the required etch depth (H) and the etch rate ratio $R\{411\}/R\{100\}$ ($\approx \delta/H$), at the concentration of the KOH solution used:

$$L = L_1 - L_2 = 2H \frac{R\{411\}}{R\{100\}} - \frac{B_{\langle 110 \rangle}}{2 \tan(30.9^\circ)} \quad 4.42$$

with H the etch depth; $B_{\langle 110 \rangle}$ the width of the $\langle 110 \rangle$ -oriented beam; $\tan(30.9^\circ)$ the geometry factor.¹⁹⁰ The factor 2 is the first term of this equation results as the etch rate of the $\{411\}$ plane is determined normal to the plane and has to be converted to the $\langle 110 \rangle$ direction. The second term in Equation 4.42 takes into account that the $\langle 110 \rangle$ beam needs to disappear completely by the time the convex corner is reached. The resulting beveling in Figure 4.63 can be reduced by further altering the compensation structures. This is done by decelerating the etch front, which largely determines the corner undercutting. One way to accomplish this is by creating more concave shapes right before the convex corner is reached. In Figure 4.61A, splitting of the compensation beam creates such concave corners, and by arranging two such double beams a more symmetrical final structure is achieved. By using these split beams, the beveling at the corner is reduced by a factor of 1.4 to 2 and leads to bevel angles under 45° .

Corner compensation with $\langle 110 \rangle$ -oriented squares (as shown in Figure 4.60A) features considerably higher spatial requirements than the $\langle 110 \rangle$ -oriented beams. Since these squares are again undercut by $\{411\}$ planes that are linked to the rugged surfaces described above, the squares do not easily lead to sharp $\{111\}$ -defined corners. Dimensioning of the compensation square is done by using Equation 4.42 again, where L_1 is half the side length of the square, and for $B_{\langle 110 \rangle}$ the side length is used. All fast-etching planes have to reach the convex corner at the same time. As before, the spatial requirements of this compensation structure can be reduced if it is combined with $\langle 110 \rangle$ -oriented beams. Such a combination is shown in Figure 4.61B. The three convex corners of the compensation square are protected from undercutting by the added $\langle 110 \rangle$ beams. During the first etch step, the $\langle 110 \rangle$ -oriented side beams are undercut by the etchant. Only after the added beams have been etched does the square itself compensate the convex corner etching. The dimensioning of this combination structure is carried out in two steps. First the $\langle 110 \rangle$ -oriented square is selected with a size that is permitted by the geometry of the device to be etched. From these dimensions, the etch depth corresponding to this size is calculated from Equation 4.42. For the remaining etch depth the $\langle 110 \rangle$ -oriented beams are dimensioned like any other $\langle 110 \rangle$ -oriented beam. If the side beam on corner b is selected about 30% longer than the other two side beams, the quality of the convex corner can be further improved. In this case, the corner is formed by the etch fronts starting at the corners a and b (Figure 4.61B).

A drawback to all the above proposed compensation schemes is the impossibility, due to rugged surfaces always accompanying $\{411\}$ planes, of obtaining a clean corner in both the top

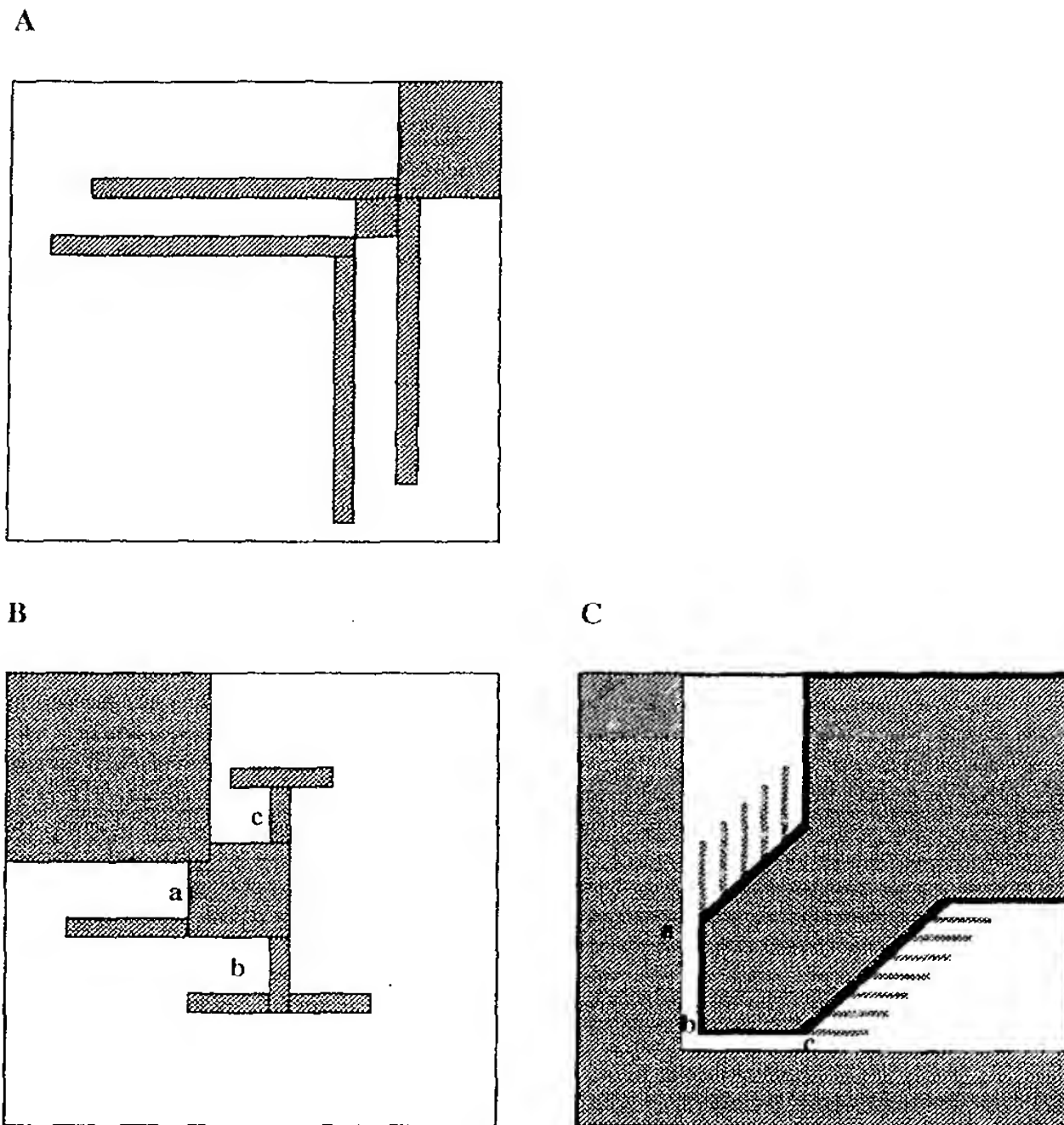


FIGURE 4.61 Mask layout for various convex corner compensation structures. (From Sandmaier, H. et al., Corner Compensation Techniques in Anisotropic Etching of (100) Silicon Using Aqueous KOH, presented at Transducers '91, San Francisco, CA, 1991. With permission.)

and the bottom of a convex edge. Buser et al.¹⁹¹ introduced a compensation scenario where a convex corner was formed by two {111} planes which were well defined all the way from the mask to the etch bottom. No rugged, undefined planes show in this case. The mask layout to create such an ideal convex corner has bands that are added to convex corners in the $\langle 100 \rangle$ direction (see Figure 4.61C and Figure 4.60 c and d). These bands will be underetched by vertical {100} planes from both sides. With suitable dimensioning of such a band, a vertically oriented membrane results, thinning, and eventually freeing the convex edge shortly before the final intended etch depth is reached. In contrast to compensation structures undercut by {411} planes, posing problems with undefined rugged surfaces (see above), this compensation structure is mainly undercut by {100} planes. Over the temperature range of 50 to 100°C and KOH concentrations ranging from 25 to 50 wt%, no undefined surfaces could be detected in the case of structures undercut by {100}

planes.¹⁸⁹ The width of these $\langle 010 \rangle$ -oriented compensation beams, which determines the minimum dimension of the structures to etch, has to be twice the etching depth. These beams can either connect two opposite corners and protect both from undercutting simultaneously, or they can be added to the individual convex corners (open beam). With an open beam approach (see Figure 4.64) one has to be certain that the {100} planes reach the corner faster than the {411} planes. For that purpose the beams have to be wide enough to avoid complete underetching by {411} planes moving in from the front side, before they are completely underetched by {100} planes moving in from the side. For instance, in a 33% KOH etchant a ratio between beam length and width of at least 1.6 is required. To make these compensation structures smaller while at the same time maintaining {100} undercutting to define the final convex corner, Sandmaier et al. remarked that the shaping {100} planes do not need to be present at the beginning of the etching

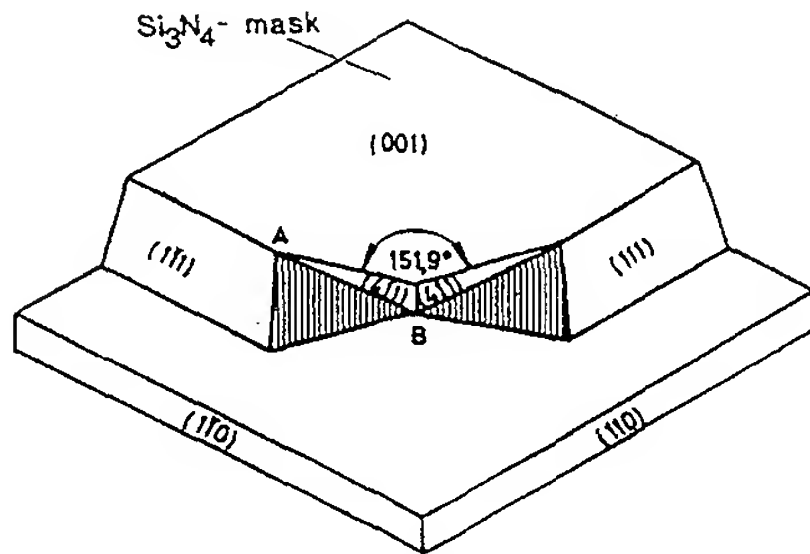


FIGURE 4.62 Planes occurring at convex corners during KOH etching. (From Mayer, G.K. et al., *J. Electrochem. Soc.*, 137, 3947–3951, 1990. With permission.)

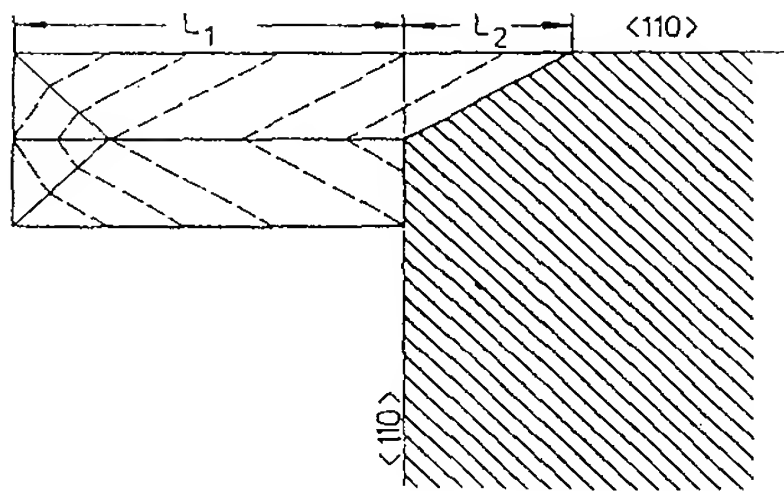


FIGURE 4.63 Dimensioning of the corner compensation structure with a $\langle 110 \rangle$ -oriented beam. (From Sandmaier, H. et al., *Corner Compensation Techniques in Anisotropic Etching of (100) Silicon Using Aqueous KOH*, presented at Transducers '91, San Francisco, CA, 1991. With permission.)

process. These authors implement delaying techniques by adding fan-like $\langle 110 \rangle$ -oriented side beams to a main $\langle 100 \rangle$ -oriented beam (see Figure 4.61C). As described above, these narrow beams are underetched by $\{411\}$ planes and the rugged surfaces they entail until reaching the $\langle 100 \rangle$ -oriented beam. Then the $\{411\}$ planes are decelerated in the concave corners between the side beams by the vertical $\{100\}$ planes with slower etching characteristics. The length of the $\langle 110 \rangle$ -oriented side beams is calculated from:

$$L_{\langle 110 \rangle} = \left(H - \frac{B_{\langle 010 \rangle}}{2} \right) \frac{R\{411\}}{R\{100\}} \quad 4.43$$

with H being the etching depth at the deepest position of the device.

The width of the side beams does not influence the calculation of their required length. In order to avoid the rugged

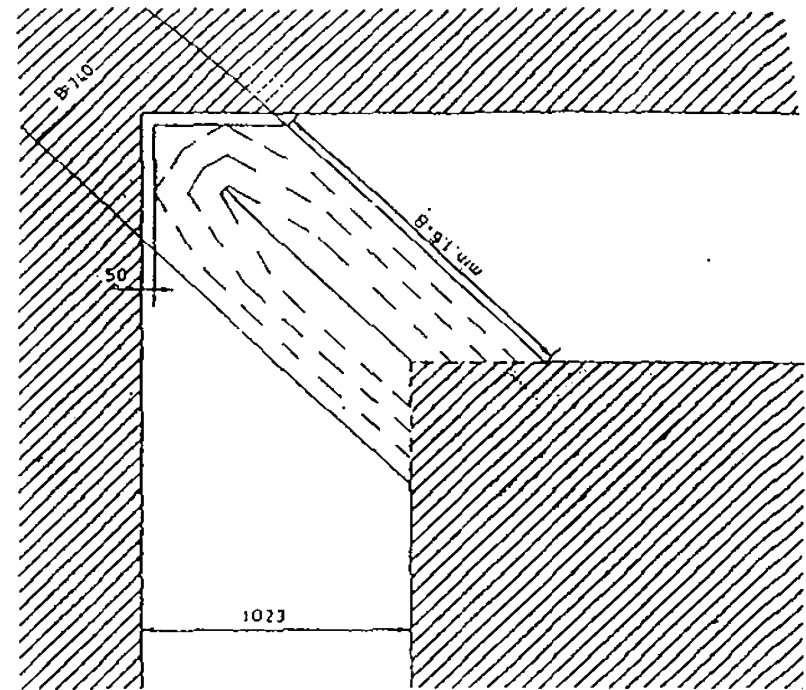


FIGURE 4.64 Beam structure open on one side. The beam is oriented in the $\langle 010 \rangle$ direction. Dimensions in microns. B is the width of the beam.

surfaces at the convex corner, the width of the side beams as well as the spaces between them should be kept as small as possible. For an etching depth of $500 \mu\text{m}$, a beam width of $20 \mu\text{m}$ and a space width of $2 \mu\text{m}$ are optimal.¹⁸⁹

Depending on the etchant, different planes are responsible for undercutting. From the above we learned that in pure KOH solutions undercutting, according to Mayer et al.¹⁹⁰ and Sandmaier et al.,¹⁸⁹ mainly proceeds through $\{411\}$ planes or $\{100\}$ planes. That the $\{411\}$ planes are the fastest undercutting planes was confirmed by Seidel;¹⁹² at the wafer surface, the sectional line of a $\{411\}$ and a $\{111\}$ plane point in the $\langle 410 \rangle$ direction, forming an angle of 30.96° with the $\langle 110 \rangle$ direction, and it was in this direction that he found a maximum in the etch rate. In KOH and EDP etchants Bean¹⁰⁵ identified the fast undercutting planes as $\{331\}$ planes. Puers et al.,¹⁸⁸ for alkali/alcohol/water, identified the fast undercutting planes as $\{331\}$ planes, as well. Mayer et al.,¹⁹⁰ working with pure KOH, could not confirm the occurrence of such planes. Lee indicated that in hydrazine-water the fastest undercutting planes are $\{211\}$ planes.⁹¹ Abu-Zeid¹⁹³ reported that the main beveling planes are $\{212\}$ planes in ethylene-diamine-water solution (no added pyrocatechol). Wu et al.¹⁹⁴ found the main beveling planes at undercut corners to be $\{212\}$ planes whether using KOH, hydrazine, or EPW solutions are used. In view of our earlier remarks on the sensitivity of etching rates of higher index rates on a wide variety of parameters (temperature, concentration, etching size, stirring, cation effect, alcohol addition, complexing agent, etc.) these contradictory results are not too surprising. Along the same line, Wu et al.¹⁹⁵ and Puers et al.¹⁸⁸ have suggested triangles to compensate for undercutting, but Mayer et al.¹⁹⁰ found them to lead to rugged surfaces at the convex corner. Combining a chemical etchant with more limited undercutting (IPA in KOH) with Sandmaier's reduced compensation structure schemes could